

Elsevier Editorial System(tm) for Computers in Biology and Medicine
Manuscript Draft

Manuscript Number: CBM-D-11-00253

Title: Real time decision support system for diagnosis of rare cancers, trained in parallel, on a graphics processing unit

Article Type: Full Length Article

Keywords: Decision Support System; Parallel Processing; Graphics Processor Unit (GPU); Rare Brain Cancers

Corresponding Author: Mr Konstantinos Sidiropoulos, MSc

Corresponding Author's Institution: Technological Educational Institute of Athens

First Author: Konstantinos Sidiropoulos, MSc

Order of Authors: Konstantinos Sidiropoulos, MSc; Dimitrios Glotsos, PhD; Spiros Kostopoulos, PhD; Panagiota Ravazoula, PhD, MD; Ioannis Kalatzis, PhD; Dionisis Cavouras, PhD; John Stonham, PhD

Abstract: In the present study a new strategy is introduced for designing and development of an efficient dynamic Decision Support System (DSS) for supporting rare cancers decision making. The proposed DSS operates on a Graphics Processing Unit (GPU) and it is capable of adjusting its design in real time based on user-defined clinical questions and of selecting the most informative histological typing criteria, in contrast to standard CPU implementations that are limited by processing and memory constrains. The proposed DSS was evaluated on 140 rare brain cancer cases on the basis of a Probabilistic Neural Network classification system, designed using a panel of 20 morphological and textural features, the exhaustive search and the leave-one-out method. Generalization was estimated using an external 10-fold cross-validation. The proposed GPU-based DSS achieved significantly higher training speed, outperforming the CPU-based system by a factor that ranged from 267 to 288 times. System design was optimized using a combination of 4 textural and morphological features with 78.6% overall accuracy, whereas system generalization was $73.8\% \pm 3.2\%$. By exploiting the inherently parallel architecture of a consumer level GPU, the proposed approach enables real time, optimal design of a DSS for any user-defined clinical question for improving diagnostic assessments, prognostic relevance and concordance rates for rare cancers in clinical practice.

Suggested Reviewers: George Sakellaropoulos PhD
Assistant Professor, Medical Physics Department, School of Medicine, University of Patras, Greece
gsak@med.upatras.gr

Antonis Daskalakis PhD
Post Doctoral Researcher, Mineral Resources Engineering, Technical University of Crete
daskalak@upatras.gr

George Nikiforidis
Professor, Department of Medical Physics, University of Patras, Greece
gnikif@med.upatras.gr

Manolis Sangriotis PhD

Associate Professor, Department of Informatics and Telecommunications, University of Athens
sagri@di.uoa.gr

Opposed Reviewers:

Conflict of Interest Statement

None declared

1
2
3
4
5
6
7
8
9
10
11
12
13
14
15
16
17
18
19
20
21
22
23
24
25
26
27
28
29
30
31
32
33
34
35
36
37
38
39
40
41
42
43
44
45
46
47
48
49
50
51
52
53
54
55
56
57
58
59
60
61
62
63
64
65

**Real time decision support system for diagnosis of rare cancers, trained in parallel, on a
graphics processing unit**

Konstantinos Sidiropoulos¹, Dimitrios Glotsos², Spiros Kostopoulos², Panagiota Ravazoula³, Ioannis
Kalatzis², Dionisis Cavouras² and, John Stonham¹

¹ School of Engineering and Design, Brunel University West London, Uxbridge, Middlesex, UB8
3PH, UK.

² Department of Medical Instruments Technology, Technological Educational Institute of Athens, Ag.
Spyridonos, Egaleo, Athens, 12210, Greece.

³ Department of Pathology, University Hospital of Patras, Rio, Patras 265 00, Greece.

Corresponding author:

Sidiropoulos Konstantinos

Medical Image and Signal Processing (medisp) Lab.

Department of Medical Instruments Technology

Technological Educational Institute of Athens,

Ag. Spyridonos Street, Egaleo, 122 10, Greece,

e-mail: Konstantinos.Sidiropoulos@brunel.ac.uk

alternative mails: ksidis@gmail.com

web site: <http://www.teiath.gr/stef/tio/medisp/index.htm>

mirror site: <http://medisp.bme.teiath.gr/>

Tel: +30 2105385375

Abstract

In the present study a new strategy is introduced for designing and developing of an efficient dynamic Decision Support System (DSS) for supporting rare cancers decision making. The proposed DSS operates on a Graphics Processing Unit (GPU) and it is capable of adjusting its design in real time based on user-defined clinical questions in contrast to standard CPU implementations that are limited by processing and memory constrains. The core of the proposed DSS was a Probabilistic Neural Network classifier and was evaluated on 140 rare brain cancer cases, regarding its ability to predict tumors' malignancy, using a panel of 20 morphological and textural features Generalization was estimated using an external 10-fold cross-validation. The proposed GPU-based DSS achieved significantly higher training speed, outperforming the CPU-based system by a factor that ranged from 267 to 288 times. System design was optimized using a combination of 4 textural and morphological features with 78.6% overall accuracy, whereas system generalization was $73.8\% \pm 3.2\%$. By exploiting the inherently parallel architecture of a consumer level GPU, the proposed approach enables real time, optimal design of a DSS for any user-defined clinical question for improving diagnostic assessments, prognostic relevance and concordance rates for rare cancers in clinical practice.

Author keywords: Decision Support System; Parallel Processing; Graphics Processor Unit (GPU); Rare Brain Cancers

1. Introduction

The majority of rare cancers are diagnosed on the basis of histological evaluation. Even though histological diagnosis is fundamentally important for patient management, the potential of diagnostic errors still remains substantially high, ranging from 25% to 40%, in routine conditions[1-3]. Factors affecting diagnostic accuracy include experts' subjectivity and lack of experience, intra and inter observer variability and poor tumor sampling; rare cancers low prevalence and their biological complexity hinder the establishment of concrete criteria able to predict tumours' behavior, and, thus, to administrate proper treatments. The latter might explain the fact that a/ although promising treatments have been proposed[4-6], death rates have not been yet reduced[4, 7-9] and b/ the cost of rare cancers management still remains one of the highest healthcare economic burdens in Europe and worldwide[10, 11]. There is a pressing need to develop methods for improving diagnostic accuracy in order to reduce diagnostic errors and, thus, guide successful choice of therapies. Accurate diagnosis linked to proper therapeutic strategies would eventually benefit patients with rare cancers improving survival and quality of life, while at the same time, keeping healthcare costs at an acceptable level.

Although it has long been recognized that a/ more resources need to be committed towards rare cancers, considering that even common types of cancer manifest multiple rare subtypes, b/ rare cancers don't conform to strict guidelines, thus experience from similar cases would improve management, c/ reproducibility in histological typing is a significant liability, since absence of well-defined criteria lead to different management decisions based on the subjective interpretation of different experts, only few studies have focused on developing new strategies for improving health care services to patients suffering from rare cancer. Research has suggested that possible solutions can be found in training and education of clinicians[12], telepathology as a result of synergistic consensus effort of several clinicians[13], and decision support systems using quantitative features extracted by image analysis[14-19].

DSS, in particular, have an increasing impact in clinical decision making based on histopathological images. A great deal of financial resources has been allocated worldwide towards promoting DSS-

1 based projects, such as the eTumour[20], and the DISHEART[21] projects. Very few projects have
2 been funded for histological and histopathological decision making (such as the EUROPATH[22], E-
3 SCOPE[23] and TUBAFROST[24] projects) and almost no integrated attempt has been made
4 towards exploiting DSS for better health care services for rare cancers. On the other hand, literature
5 shows piecemeal approaches on the basis of DSS focusing on specific subtypes of rare tumors, such
6 as astrocytomas, glioblastomas, meningiomas and atypical metastatic cancers[14-19]. Although such
7 attempts have highlighted the contribution of DSS in improving diagnostic assessments, prognostic
8 relevance and concordance rates, the exploitation of such systems in clinical practice is limited due to
9 the following reasons: First, proposed DSS have been designed to focus on specific groups (two or
10 three class problems) of rare cancers[14-19]. However, the exact classification of each type of rare
11 tumor is, in most cases, a result of an exhaustive search from a list of multiple possible outcomes
12 based on the cell type of origin of the disease (for example the new World Health Organization
13 classification of tumors affecting the central nervous system defining 9 categories of neuroepithelial
14 tumors, each of which has subcategories dictating choice of therapy and prognosis[25]). Second,
15 reliable DSS require a considerable number of cases for learning and designing of the prediction
16 rules. However, due to the low prevalence of rare cancers[26], it is difficult to collect large datasets
17 that will ensure reliability in decision making. Third, quantitative descriptor of tumoral microscopic
18 images comprises a large list of structural, morphological, textural and ordinal assessments. The
19 effective selection of the most informative of these descriptors would require an exhaustive search
20 among all possible combinations. However, exhaustive search is limited by serious computational
21 and memory limitations.

22
23
24
25
26
27
28
29
30
31
32
33
34
35
36
37
38
39
40
41
42
43
44
45
46
47
48
49 In the present study a new strategy is introduced for designing and developing of an efficient dynamic
50 decision support system for supporting rare cancers decision making. The proposed DSS is built on a
51 Graphics Processing Unit (GPU) framework and it is capable of updating its structure in real time
52 whenever a new verified case is uploaded on its repository. Moreover, the system adjusts its design
53 based on the exact clinical question to be answered, which is user-defined from on a list of potential
54 outcomes according to existing clinical classifications. Finally, the GPU-framework enables the
55
56
57
58
59
60
61
62
63
64
65

1 optimal selection of the most informative histological typing criteria, in contrast to standard CPU
2 implementations that are limited by processing and memory constrains. In this way, it is possible to
3
4 examine exhaustively a significant larger panel of quantitative histological descriptors combining
5
6 structural, textural and morphological information, something that is unrealistic on standard CPU
7
8 implementations. The proposed DSS was evaluated on rare brain cancer cases.
9

10
11
12
13
14
15
16
17
18
19
20
21
22
23
24
25
26
27
28
29
30
31
32
33
34
35
36
37
38
39
40
41
42
43
44
45
46
47
48
49
50
51
52
53
54
55
56
57
58
59
60
61
62
63
64
65

2. Material and Methods

2.1 Material

Clinical material comprised 140 cases of rare brain tumors, including astrocytomas (variants: gemistocytic, fibrillary and mixed), anaplastic astrocytomas, glioblastomas, oligodendroglioma and mixed gliomas. At least three Hematoxylin-Eosin (H&E) stained sections were generated from the same block of formalin-fixed paraffin-embedded tissue for each case (patient). The type and the degree of malignancy (grade) of each tumor was defined according to the WHO guidelines for classification of neuroepithelial tumors of the central nervous system[25]. Of the 140 cases, 61 were characterized as grade II (aggressive), 35 as grade III (more aggressive) and 44 as grade IV (most aggressive). Each grade category consisted of subtypes listed in Table 1.

Five images for each case were digitized based on the guidelines of an experienced histopathologist (P.R.). The digitization was performed using a light microscopy imaging system consisted of a Zeiss Axiostar-Plus microscope (ZEISS; Germany) connected to a Leica DC 300 F color video camera (LEICA; Germany).

2.2 Methods

Images were converted to greyscale for further processing. A pixel-based classification algorithm presented by our group elsewhere[27] was used to isolate nuclei from surrounding tissue. An example of an original and a segmented image of a grade IV pleomorphic glioblastoma multiforme is illustrated at Figure 1a and 1b respectively. Segmented nuclei were quantified by means of 20 textural and morphological features describing the size, shape and grain texture of nuclei. The list of the features computed is presented at Figure 2. The latter features have been shown of diagnostic and prognostic significance in grading and typing of brain tumors[15, 18].

The pattern recognition system was designed with a Probabilistic Neural Network (PNN)[28]

1 classifier with Gaussian kernel (the spread of the Gaussian kernel was experimentally determined
2 equal to 0.2), the leave-one-out[29] and the exhaustive search[30] to estimate the resubstitution error
3 and based on this error select the most informative features. An external 10-fold cross validation
4 process was employed for estimating the generalization of the prediction rule to unknown cases.
5
6 According to the external cross validation data were randomly split into 10 different non-overlapping
7 subsets. At each stage of the cross validation the leave-one-out and the exhaustive search method was
8 implemented to 9 datasets, external to the tenth test subset. The average external cross validation
9 error was calculated over 50 such random splits.
10
11
12
13
14
15
16
17
18

19 In order to adapt the training of the aforementioned classifier to the inherently parallel SIMD
20 (Single Instruction Multiple Data) architecture of a GPU, the whole procedure was broken into many
21 tasks that were designed to run concurrently. In technical terms, the challenge was to design the
22 kernel, or the small code fragment running in multiple parallel threads, in an optimal way in order to
23 evenly distribute the workload and maximize performance. It should be noted that in the present
24 study NVIDIA's Compute Unified Device Architecture (CUDA)[19] version 4.0 programming
25 framework was selected and utilized, mainly due to its maturity.
26
27
28
29
30
31
32
33
34
35

36 In the proposed implementation, the first step involved the enumeration of all possible feature
37 combinations. Following the transfer of the training dataset from the memory of the host PC to the
38 GPU's global memory, each thread was assigned with a single feature combination (Figure 3).
39 Specifically, the task of each thread, running concurrently, was to train the PNN classifier with this
40 unique feature combination and evaluate its classification accuracy by means of the leave-one-out
41 technique. Hence, for a given training dataset consisting of N patterns, every thread trained the PNN
42 classifier N times for a single combination of features, but each time leaving another pattern out of
43 the training set. It should be noted that feature combinations were transferred to the device memory
44 for processing in batches of 80000 combinations. Upon completion of all threads, results were
45 transferred back to the host's memory for presentation (Figure 4). Listing 1 shows the kernel function
46 executed by each CUDA thread. Block and Grid size were experimentally set to [128 x 1] and [625 x
47
48
49
50
51
52
53
54
55
56
57
58
59
60
61
62
63
64
65

1 x 1] respectively.

1
2
3 In order to evaluate its performance, the developed GPU-based DSS was trained in a series of
4 experiments and the required training time was measured. The latter was then compared with the
5 respective training time of the same classifier running on a typical CPU and programmed in C
6 programming language. Two series of experiments were performed in order to investigate the impact
7 of both a/feature dimensionality and b/dataset size in training time. Hence, regarding the first series
8 of experiments, both systems were trained with a dataset, consisting of 140 patterns that
9 progressively increased their feature dimensions, beginning with 14 features and reaching 20 by a
10 step of 2. In the second series of experiments the two systems were trained with a 20-feature dataset
11 that progressively increased its size, by adding more patterns. Therefore, beginning with 80 patterns,
12 the dataset steadily increased its size to 140 patterns by steps of 10.
13
14
15
16
17
18
19
20
21
22
23
24
25
26

27 All experiments were performed on a desktop PC featuring an Intel Core 2 Quad CPU at
28 2.83GHz, and hosting a GeForce GTX 580. The hardware specification of the proposed method
29 experimental setup is illustrated in Tables A1 and A2 (see APPENDIX A).
30
31
32
33
34
35
36
37
38
39
40
41
42
43
44
45
46
47
48
49
50
51
52
53
54
55
56
57
58
59
60
61
62
63
64
65

3. Results

The first series of experiments attempted to investigate the impact of feature dimensionality in the performance of the proposed DSS. Table 2 illustrates the computation time measured by both the GPU and the CPU-based systems. As far as the GPU is concerned, total processing time includes also the time required for memory transfers between the host's and the GPU's memory. As one can easily observe, the proposed GPU-based PNN classifier system achieved significantly higher training speed in all cases, outperforming the CPU-based system by a factor that ranged from 267.1 to 288.9 times (Figure 5). In case of exhaustive combination of 20 features, which translates to 1048575 distinct feature combinations, the CPU-based system required about 6.5 hours while the GPU-based system completed training in just 85 seconds .

The purpose of the second series of experiments was to assess the effect of the dataset size on the required training time of the proposed GPU-based DSS. According to the results, presented in Table 3 and illustrated in Figure 6, training time of both systems is increased at almost the same rates, with the GPU-based DSS outperforming the CPU-based system by a factor that ranged from 278.5 to 279.4 times.

It should be noted, that in all experiments performed, transfer time varied between 0.17% and 0.50% of total training time depending on the number of features combined and the number of patterns constituting the training set.

According to the exhaustive search and the LOO method, the proposed GPU-based DSS gave optimum results in the discrimination of low from high grade rare brain tumors using 4 features: low grade cases were correctly identified with 72.1%, high grade cases with 83.5% whereas the overall accuracy achieved was 78.6%. The performance of the system for different number of feature combinations is illustrated in Figure 7. Applying the external 10-fold cross-validation method, overall accuracy was $73.8\% \pm 3.2\%$.

4. Discussion

DSS have been proven as important second opinion tools for reducing inter-observer reliability and diagnostic misinterpretations in diagnostic pathology[31-33]. Considering that accurate histological diagnosis leads to more precise treatment planning in rare cancers, DSS, as well as other tools contributing towards this direction, are of crucial importance in improving chances of survival of patients. Although piecemeal research efforts have been presented in literature regarding DSS for rare cancers [14-19], their application into clinical practice is limited due to the following reasons: a/ available data are limited due to low prevalence of such diseases; small sample sizes are prohibitive for designing reliable DSS. b/ rare cancers recognition is a multiclass problem; it is very difficult to build a DSS system able to identify all possible outcomes of any type of rare cancer, since it would require a significant amount of data for each subtype of tumor whose identification is of clinical importance. c/ quantitative descriptors extracted from biopsy images include a panel of structural, textural, morphological and qualitative expert-based ordinal scales. The optimal selection of the best subset of these descriptors would require exhaustive search algorithms to seek all possible combinations. However, the running time of an exhaustive search is proportional to the dimension and size of the dataset. An exhaustive search within 20 features for 140 data with the leave-one-out method would require the designing of more than 140 million classifiers. In practice common pattern recognition applications employ much less than 20 features in exhaustive search and stop the search at combinations of up to 7-8 due to memory and CPU restrictions.

One of the solutions proposed, so as to tackle the aforementioned problem, is parallel processing typically involving powerful supercomputers, or server clusters. Unfortunately, this kind of hardware is expensive and therefore accessible only to few people. However, a new promising development in this regard is the emergence of consumer-level graphics processing units (GPUs) as a mainstream computing platform[34].

Previous studies in the field of image processing and analysis that attempt to benefit in speed from the utilization of GPUs, include implementations of neural networks[35], Kernel methods for Support

1 Vector Machine classifiers[36], k-Nearest Neighbor search methods[37], and algorithms for both
2 computed tomography reconstruction[34] and registration of medical images[38, 39]. In another
3 study[40], Ruiz A. et al proposed a GPU-based CAP system for prognosis of neuroblastoma
4 achieving 45 times faster execution time compared to a CPU based system.
5
6

7
8
9 The proposed DSS offers solutions to the above problems. First, it is designed using an external
10 cross-validation process to ensure generalization to unseen data[41]. External cross validation is the
11 most plausible candidate method in cases where we don't have the luxury of withholding a part of
12 data for testing. In this way, two goals are achieved: the DSS can be designed with limited data,
13 which is the case in rare cancers, while safeguarding that success rates will apply to new cases.
14 Moreover, the system can be re-designed in real time when new verified cases are added to its
15 repository increasing, in this way, the sample size and the experience of the system in predicting
16 clinical meaningful subcategories. The time needed to design the system for 140 cases on a CPU
17 required 6.5 hours, whereas in for the GPU-framework it took around 1.4 minutes (see Table 2 or
18 Figure 5). Second, the fast and dynamic implementation on the GPU-framework enables the expert to
19 define the exact categories that need to be separated. In most rare cancers diagnostic difficulties arise
20 from problems of tumoral biological continuum; thus, the degeneration of the multi-class problem to
21 two-class differential diagnosis problem is a reasonable assumption. Under this framework, the
22 expert physician may design in real time a DSS for separation of any subtype of rare cancers using
23 the same dataset. From Table 3 or Figure 6 it can be observed that the GPU is more than 278 times
24 faster than the CPU, enabling, in this way, real time exploitation of the system. Third, it is possible to
25 investigate the performance of higher dimension datasets on the basis of the optimal exhaustive
26 search method. In this way, the expert may review the predictive value of complementary information
27 from different origin tumoral descriptors, such as textural, morphological, structural and ordinal
28 descriptors. In the experiments for brain tumor grade determination optimum results (78.6%) were
29 obtained using combinations of 4 features (concavity, density, energy and inertia). Higher features
30 combinations resulted in inferior prediction rates. This result was anticipated since as the number of
31 features increases for fix sample size, data become sparse and the curse of dimensionality
32
33
34
35
36
37
38
39
40
41
42
43
44
45
46
47
48
49
50
51
52
53
54
55
56
57
58
59
60
61
62
63
64
65

1 predominates. The rule of thumb indicates that the ratio of dataset size to the number of features
2 should not fall under 20[42]; this was experimentally verified since in our case best results were
3
4 obtained for the low grade class when the aforementioned ratio was equal to 20.3 (61 cases and 3
5
6 features), whereas for the high grade class when the respective ratio was 19.8 (79 cases and 4
7
8 features) (see Figure 7). The latter is a key observation regarding the need to re-train the DSS each
9
10 time a new batch of cases is added to its repository. Re-training on larger sample sizes would
11
12 potentially enable the identification of an even larger feature subset of improved performance than
13
14 those already identified, without being limited by peaking phenomena effects. In this way, the
15
16 investigation of complementary information of different origin features would be feasible.
17
18
19
20

21 To test the generalization of the proposed method to new data, a 10-fold external cross-validation
22
23 procedure was applied, giving estimates up to $73.8\% \pm 3.2\%$ overall accuracy. The reduced
24
25 performance of the system under the external cross validation process is expected since the leave-
26
27 one-out method leads to optimistically biased estimates of the classifier performance. The leave-one-
28
29 out method can be used for efficient classifier design by means of selecting most informative features
30
31 and best settings for the prediction rule; however, if one seeks to estimate the generalization
32
33 capability of the prediction rule to unseen cases, then the external validation rate is more realistic
34
35 than the leave-one-out rate.
36
37
38
39
40
41
42
43
44

45 **Acknowledgements**

46
47 The first author was supported by a grant from the Greek State Scholarships Foundation (IKY).
48
49
50
51
52
53
54
55
56
57
58
59
60
61
62
63
64
65

References

1. C. Fletcher: Diagnostic histopathology of tumors, (New York : Churchill Livingstone, Edinburgh, 1995).
2. A. D. Ramsay, Errors by locums. Histopathology departments already audit diagnostic errors, British Medical Journal 313 (1996) 117.
3. D. B. Troxel, Diagnostic Errors in Surgical Pathology Uncovered by a Review of Malpractice Claims. Part III. Breast Biopsies, International journal of surgical pathology 8 (2000) 335-337.
4. F. Cowie, Treatment of rare cancers: gastrointestinal stromal tumours, British Journal of Hospital Medicine 67 (2006) 361-4.
5. J. Gonzalez and Gilbert, M. R., Treatment of astrocytomas, Current opinion in neurology 18 (2005) 632-8.
6. W. E. Longo, Vernava, A. M., 3rd, Wade, T. P. et al., Rare anal canal cancers in the U.S. veteran: patterns of disease and results of treatment, The American surgeon 61 (1995) 495-500.
7. J. A. DiSario, Colorectal cancers of rare histologic types compared with adenocarcinomas, Diseases of the colon and rectum 38 (1995) 1227.
8. A. Dixon, Rare skin cancers in general practice, Australian family physician 36 (2007) 141-3.
9. T. Joannides, Rare cancers, Clinical Oncology 13 (2001) 235.
10. Y. Belkacemi, Zouhair, A., Ozsahin, M., Azria, D. and Mirimanoff, R. O., [Prognostic factors and management of rare cancers], Cancer/Radiothérapie 10 (2006) 323-9.
11. L. Kutikova, Bowman, L., Chang, S. et al., Utilization and cost of health care services associated with primary malignant brain tumors in the United States, Journal of neuro-oncology 81 (2007) 61-5.
12. RA Prayson, Agamanolis, DP, Cohen, ML et al., Interobserver reproducibility among neuropathologists and surgical pathologists in fibrillary astrocytoma grading, J NEUROL SCI 175 (2000) 33-39.
13. W. Coons, Jhonson, P., Sceithauer, B., Yates, A. and Pearl, D., Improving diagnostic accuracy and interobserver concordance in the classification and grading of Primary Gliomas, Cancer 79 (1997) 1381-93.
14. N. Belacel and Boulassel, M., Multicriteria fuzzy assignment method: a useful tool to assist medical diagnosis, Artificial intelligence in medicine 21 (2001) 201-207.
15. C. Decaestecker, Camby, I., Nagy, N. et al., Improving morphology-based malignancy grading schemes

- in astrocytic tumors by means of computer-assisted techniques, *Brain Pathology* 8 (1998) 29-38.
16. Guo-Zheng Li, Yang, Jie, Ye, Chen-Zhou and Geng, Dao-Ying, Degree prediction of malignancy in brain glioma using support vector machines, *Computers in Biology and Medicine* 36 (2006) 313-325.
 17. R Nafe, W Schlote and Schneider, B, Histomorphometry of tumour cell nuclei in astrocytomas using shape analysis, densitometry and topometric analysis, *Neuropathology Applied Neurobiology* 31 (2005) 34-44
 18. P. K. Sallinen, Sallinen, S. L., Helen, P. T. et al., Grading of diffusely infiltrating astrocytomas by quantitative histopathology, cell proliferation and image cytometric DNA analysis. Comparison of 133 tumours in the context of the WHO 1979 and WHO 1993 grading schemes, *Neuropathology and applied neurobiology* 26 (2000) 319-31.
 19. M. Scarpelli, Montironi, R., Thompson, D. and Bartels, P., Computer-Assisted Discrimination of Glioblastomas, *Analytical and Quantitative Cytology and Histopathology* 19 (1997) 369-375.
 20. eTumour, <http://www.ist-world.org/ProjectDetails.aspx?ProjectId=ec81f1ded2ff4c82a6573cc77f2a3c79>
 21. DISHEART, <http://www.ist-world.org/ProjectDetails.aspx?ProjectId=2916094e804346ecbffc9d9a45fe9cf8>
 22. EUROPATH, <http://telescan.nki.nl/action/europath.htm>
 23. E-SCOPE, http://cordis.europa.eu/fetch?CALLER=PROJ_ICT&ACTION=D&CAT=PROJ&RCN=71240
 24. TUBAFROST, <http://www.tubafrost.org/>
 25. A. Rousseau, Mokhtari, K. and Duyckaerts, C., The 2007 WHO classification of tumors of the central nervous system - what has changed?, *Current opinion in neurology* 21 (2008) 720-7.
 26. Paolo G. Casali, Do rare cancers deserve specific strategies for cancer research?, *The Lancet Oncology* 11 506-507.
 27. D. Glotsos, Spyridonos, P., Cavouras, D. et al., Automated segmentation of routinely hematoxylin-eosin-stained microscopic images by combining support vector machine clustering and active contour models, *Analytical & Quantitative Cytology & Histology* 26 (2004) 331-40.
 28. D.F. Specht, Probabilistic Neural Networks, *Neural Networks* 3 (1990) 109-118.
 29. P. A. Lachenbruch, An almost unbiased method of obtaining confidence intervals for the probability of misclassification in discriminant analysis, *Biometrics* 23 (1967) 639-45.

- 1
2
3
4
5
6
7
8
9
10
11
12
13
14
15
16
17
18
19
20
21
22
23
24
25
26
27
28
29
30
31
32
33
34
35
36
37
38
39
40
41
42
43
44
45
46
47
48
49
50
51
52
53
54
55
56
57
58
59
60
61
62
63
64
65
30. J. Fellow, Duin, R. and Mao, J., Statistical pattern recognition: A review, *IEEE Transactions on pattern analysis and machine intelligence* 22 (2000) 4-37.
 31. Dorin Comaniciu, Bogdan Georgescu, Peter Meer, Wenjin Chen and Foran, David. *Decision Support System for Multiuser Remote Microscopy in Telepathology IEEE Symposium on Computer-Based Medical Systems* 1999
 32. R. Logeswaran, Cholangiocarcinoma--an automated preliminary detection system using MLP, *Journal of medical systems* 33 (2009) 413-21.
 33. P. Spyridonos, Cavouras, D., Ravazoula, P. and Nikiforidis, G., A computer-based diagnostic and prognostic system for assessing urinary bladder tumour grade and predicting cancer recurrence, *Medical Informatics and the Internet in Medicine* 27 (2002) 111-22.
 34. F. Xu and Mueller, K., Real-time 3D computed tomographic reconstruction using commodity graphics hardware, *Physics in medicine and biology* 52 (2007) 3405-19.
 35. Oh. Kyoung-Su and Keechul, Jung., GPU implementation of neural networks, *Pattern Recognition* 37 (2004) 1311-1314.
 36. Julius. Ohmer, Maire, Frederic. and Brown, Ross., *Implementation of Kernel Methods on the GPU Digital Imaging Computing: Techniques and Applications (DICTA 2005)* 2005
 37. Vincent. Garcia, Debreuve, Eric. and Barlaud, Michel. (2008) Fast k nearest neighbor search using GPU *IEEE Computer Society Conference on Computer Vision and Pattern Recognition Workshops, 2008. CVPRW '08.* (Anchorage, AK).
 38. R. Shams, Sadeghi, P., Kennedy, R. and Hartley, R., Parallel computation of mutual information on the GPU with application to real-time registration of 3D medical images, *Computer methods and programs in biomedicine* (2009)
 39. R. J. Lapeer, Shah, S. K. and Rowland, R. S., An optimised radial basis function algorithm for fast non-rigid registration of medical images, *Computers in Biology and Medicine* 40 (2010) 1-7.
 40. A. Ruiz, Sertel, O., Ujaldon, M. et al., Stroma classification for neuroblastoma on graphics processors, *International journal of data mining and bioinformatics* 3 (2009) 280-98.
 41. C. Ambrose and McLachlan, G. J., Selection bias in gene extraction on the basis of microarray gene-expression data, *Proceedings of the National Academy of Sciences of the United States of America* 99 (2002) 6562-6566.
 42. V. Kechman, *Learning and Soft Computing*, p. 121-184. (2001).

1
2
3
4
5
6
7
8
9
10
11
12
13
14
15
16
17
18
19
20
21
22
23
24
25
26
27
28
29
30
31
32
33
34
35
36
37
38
39
40
41
42
43
44
45
46
47
48
49
50
51
52
53
54
55
56
57
58
59
60
61
62
63
64
65

FIGURE LEGENDS

1
2 Figure 1a: An example of a high grade pleomorphic glioblastoma multiforme tumor.
3
4

5
6 Figure 1b: Segmentation of Figure 1a for isolation of nuclei from surrounding tissue
7
8

9
10 Figure 2: Morphological, textural and structural tumoral quantitative descriptors
11
12

13 Figure 3: Parallel training of the proposed GPU-based DSS distributed to N threads, where
14 each GPU thread was assigned with the training of a PNN classifier for a unique feature
15 combination.
16
17

18
19
20
21 Figure 4: The task of each thread, running concurrently, was to train the PNN classifier with a
22 unique feature combination and evaluate its classification accuracy by means of the leave-
23 one-pattern-out technique. In every case the output of each thread was the overall accuracy
24 achieved for the specific feature combination.
25
26
27

28
29
30 Figure 5: Comparative assessment of CPU and GPU regarding training time of the DSS
31 versus the dataset's feature dimensionality (the x-axis is presented in logarithmic scale)
32
33
34

35
36 Figure 6: Comparative assessment of CPU and GPU regarding training time of the DSS
37 versus the dataset's size (the x-axis is presented in logarithmic scale)
38
39
40

41 Figure 7: Success rates of the proposed GPU-based DSS in the discrimination of low from
42 high grade rare brain tumors.
43
44
45
46
47
48
49
50
51
52
53
54
55
56
57
58
59
60
61
62
63
64
65

LISTINGS

Listing 1: The kernel used to design the proposed DSS

```
1
2
3
4
5
6
7
8
9
10 1  __global__ void
11 2  GPUSingleCombination_LOO_PNN(
12 3  // Pointer to the dataset stored in global memory
13 4  float* features,
14 5  // Pointer to the mean values lookup table stored in global memory
15 6  float* meanFeatures,
16 7  // Pointer to the standard deviations lookup table stored in global memory
17 8  float* stdvFeatures,
18 9  // Size of dataset - Number of patterns
19 10 int D_SIZE,
20 11 // Defines the point in dataset where class 2 begins
21 12 int CDIVIDER,
22 13 // Max number of features
23 14 int P_SIZE ,
24 15 // Pointer to all possible feature combinations stored in global memory
25 16 int* combination ,
26 17 // Pointer to the size of each feature combination
27 18 int* combinationSize,
28 19 // Pointer to an array used to store the overall accuracy
29 20 // for each possible feature combination
30 21 float* overallAccuracy )
31 22 {
32 23     //Unique thread identifier
33 24     int index = (blockIdx.x * 128) + threadIdx.x;
34 25     //Various variables
35 26     int i, k, c1;
36 27     unsigned int  combK;
37 28     float unknownP[22];
38 29     int class1Count, class2Count;
39 30
40 31     float p = 2.0f;
```

```

32     float sigma = 0.2f;
1 33     float pi = 3.14159f;
2
3 34     float distance, distanceInP;
4
5 35     float denominator = 2.0f * powf(sigma,2);
6
7 36     float denominatorP = 0.0f;
8
9 37     float tempSum, tempExpSum, expvar;
10
11 38     int classSelected=0;
12
13 39     float g1 = 0.0;
14
15 40     float g2 = 0.0;
16
17 41     int truthTable[2][2];
18
19 42     truthTable[0][0] =0;
20
21 43     truthTable[0][1] =0;
22
23 44     truthTable[1][0] =0;
24
25 45     truthTable[1][1] =0;
26
27
28 46
29
30 47     //Get the size of the specific combination
31
32 48     unsigned int COMBINATION_SIZE = combinationSize[index];
33
34
35 49
36
37 50     // For all patterns
38
39 51     // Apply Leave one out method
40
41 52     for(i=0; i<D_SIZE; i++){
42
43 53
44
45 54         classSelected=1;
46
47 55         if(i<CDIVIDER)
48
49 56             classSelected=0;
50
51 57         //If 0 then patterns belongs to Class 1 else it belongs to Class 2
52
53 58         // Copy unknown pattern from global memory and normalize it
54
55 59         for(k=0; k<P_SIZE; k++){
56
57 60             unknownP[k] = ( features[(i * P_SIZE) + k]
58
59 61                 - meanFeatures[(i * P_SIZE) + k] ) / (float) stdvFeatures[(i * P_SIZE) + k];
60
61 62         }
62
63 63         // Calculate discriminant PNN function for Class 1
64
65 64         class1Count = 0;
66
67 65         tempExpSum = 0.0;
68
69 66         for(c1=0; c1<CDIVIDER; c1++) {
70
71 67
72
73 68             if(c1!=i){ // NOT the left-out pattern
74
75 69
76
77 70
78
79 71
80
81 72
82
83 73
84
85 74
86
87 75
88
89 76
90
91 77
92
93 78
94
95 79
96
97 80
98
99 81
100

```

```

69         class1Count++;
1 70         // Calculate square distance
2
3 71         tempSum = 0.0;
4
5 72         for(k=0; k<COMBINATION_SIZE; k++){
6 73             combK = combination[ (index * P_SIZE) + k ];
7
8 74             distance = unknownP[ combK ] - ( ( features[ (c1 * P_SIZE) + combK ] -
9
10 75                 meanFeatures[ (i * P_SIZE) + combK ] ) / (float)
11 76                 stdvFeatures[ (i * P_SIZE) + combK ] );
12
13 77             distanceInP = powf( distance , 2);
14
15 78             tempSum = tempSum + distanceInP;
16
17 79         }
18 80         expvar = expf( - tempSum/denominator);
19
20 81         tempExpSum = tempExpSum + expvar;
21
22 82
23 83     }//if(c1!=i)
24
25 84
26 85 }
27
28 86
29
30 87 denominatorP = powf( 2.0f * pi , (COMBINATION_SIZE/2) ) * powf( sigma , COMBINATION_SIZE);
31
32 88 g1 = tempExpSum / ( denominatorP * class1Count);
33
34 89 // Calculate discriminant PNN function for Class 2
35
36 90 class2Count = 0;
37
38 91 tempExpSum = 0.0;
39
40 92 for(c1=CDIVIDER; c1<D_SIZE; c1++) {
41 93     if(c1!=i){ // NOT the left-out pattern
42 94         class2Count++;
43 95         // Calculate square distance
44
45 96         tempSum = 0.0;
46
47 97         for(k=0; k<COMBINATION_SIZE; k++){
48 98             combK = combination[ (index * P_SIZE) + k ];
49
50 99             distance = unknownP[ combK ] - ( ( features[ (c1 * P_SIZE) + combK ] -
51
52 100                 meanFeatures[ (i * P_SIZE) + combK ] ) / (float)
53 101                 stdvFeatures[ (i * P_SIZE) + combK ] );
54
55 102             distanceInP = powf( distance , 2);
56
57 103             tempSum = tempSum + distanceInP;
58
59 104         }
60 105         expvar = expf( - tempSum/denominator);
61
62
63
64
65

```

```

106         tempExpSum = tempExpSum + expvar;
1
2 107
3 108         }//if(c1!=i)
4
5 109     }
6
7 110     denominatorP = powf( 2.0f * pi , (COMBINATION_SIZE/2) ) * powf( sigma , COMBINATION_SIZE);
8
9 111     g2 = tempExpSum / ( denominatorP * class2Count);
10
11 112     //Fill up the truth table
12
13 113     if(g1>=g2){
14
15 114         truthTable[classSelected][0]++;
16
17 115     }
18
19 116     else{
20
21 117         truthTable[classSelected][1]++;
22
23 118     }
24
25 119 }
26
27 120 //Calculate OverallAccuracy for this feature combination
28
29 121 float OverallAccuracy = 0.0f;
30
31 122 OverallAccuracy = (truthTable[0][0] + truthTable[1][1]) * 100
32
33 123     / (truthTable[0][0] + truthTable[0][1] + truthTable[1][0] + truthTable[1][1] );
34
35 124 //Update the value in global memory
36
37 125 overallAccuracy[index] = OverallAccuracy;
38
39 126 //Wait for all threads to reach this point
40
41 127 __syncthreads();
42
43 128 }
44
45
46
47
48
49
50
51
52
53
54
55
56
57
58
59
60
61
62
63
64
65

```

APPENDIX A

Table A1: Specifications of the host PC

Host hardware specification	
Processor	Intel Core 2 Quad, 2.83GHz
Memory	4GB DDR3
Motherboard	ASUSTeK P5Q3
Operating System	Windows 7 Ultimate 32bit

Table A2: Specifications of GPU device

GPU specification	
Model	GeForce GTX 580
Number of multiprocessors	16
Number of CUDA cores	512
Total global memory	1472 MB GDDR5
Shared memory per block	48 KB
Memory interface width	384 bits
Memory clock speed	4200 MHz
Warp size	32
Core clock speed	832 MHz
CUDA compute capability	2.0

TABLES

Table 1: Brain tumors dataset

Astrocytoma (WHO grade II)			Astrocytoma (WHO grade III)		Glioblastoma multiforme (WHO grade IV)		
Gemistocytic	Fibrillary	Mixed	Anaplastic	Anaplastic mixed	Giant cell	Gliosarcoma	Pleomorphic
8	19	34	25	10	13	1	30
61			35		44		

Table 2: Impact of dataset's feature dimension in designing the PNN classifier using the exhaustive search and the leave-one-out methods

Total number of features exhaustively combined	Number of distinct feature combinations	PNN Training Time for 140 patterns (ms)				CPU/GPU Training. Time
		CPU	GPU			
			Processing	Transfer	Total	
14	16383	266696	994.50	4.01	998.51	267.1
16	65535	1202711	4164.91	10.88	4175.79	288.0
18	262143	5351447	18475.58	46.75	18522.33	288.9
20	1048575	23557518	84421.21	139.76	84560.97	278.6

Table 3: Impact of dataset's size in designing the PNN classifier using the exhaustive search and the leave-one-out methods

Number of Patterns	PNN Training Time (ms)				CPU/GPU Training Time
	CPU	GPU			
		Processing	Transfer	Total	
80	7695287	27455.52	138.64	27594.16	278.9
90	9756267	34786.87	137.40	34924.27	279.4
100	12010644	42946.45	137.65	43084.10	278.8
110	14544027	52083.37	138.32	52221.69	278.5
120	17306957	61887.07	136.92	62023.99	279.0
130	20289976	72725.09	138.77	72863.86	278.5
140	23557518	84421.21	139.76	84560.97	278.6

Figure 1a
[Click here to download high resolution image](#)

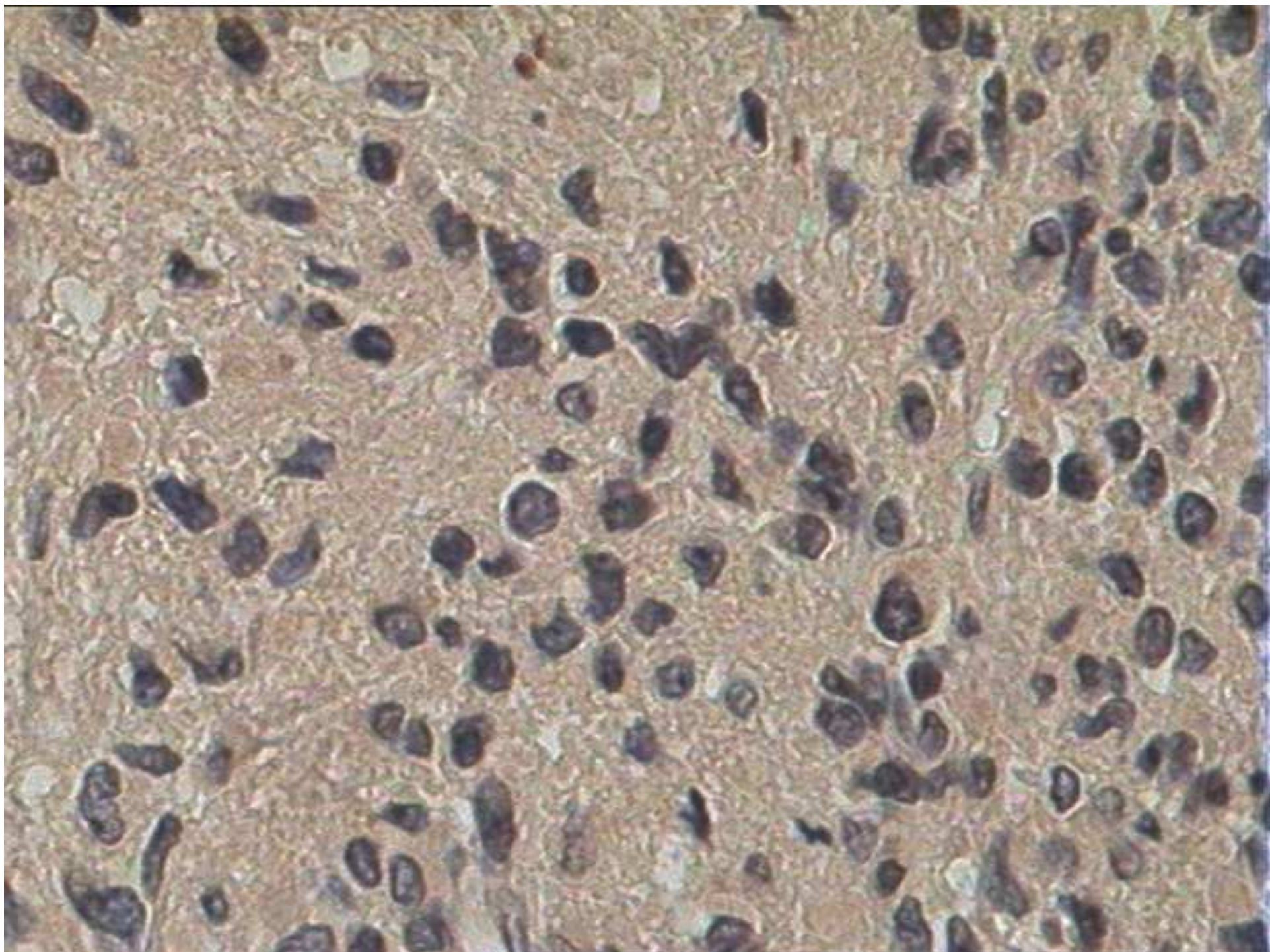


Figure 1b
[Click here to download high resolution image](#)



Figure 2
[Click here to download high resolution image](#)



Figure 3
[Click here to download high resolution image](#)

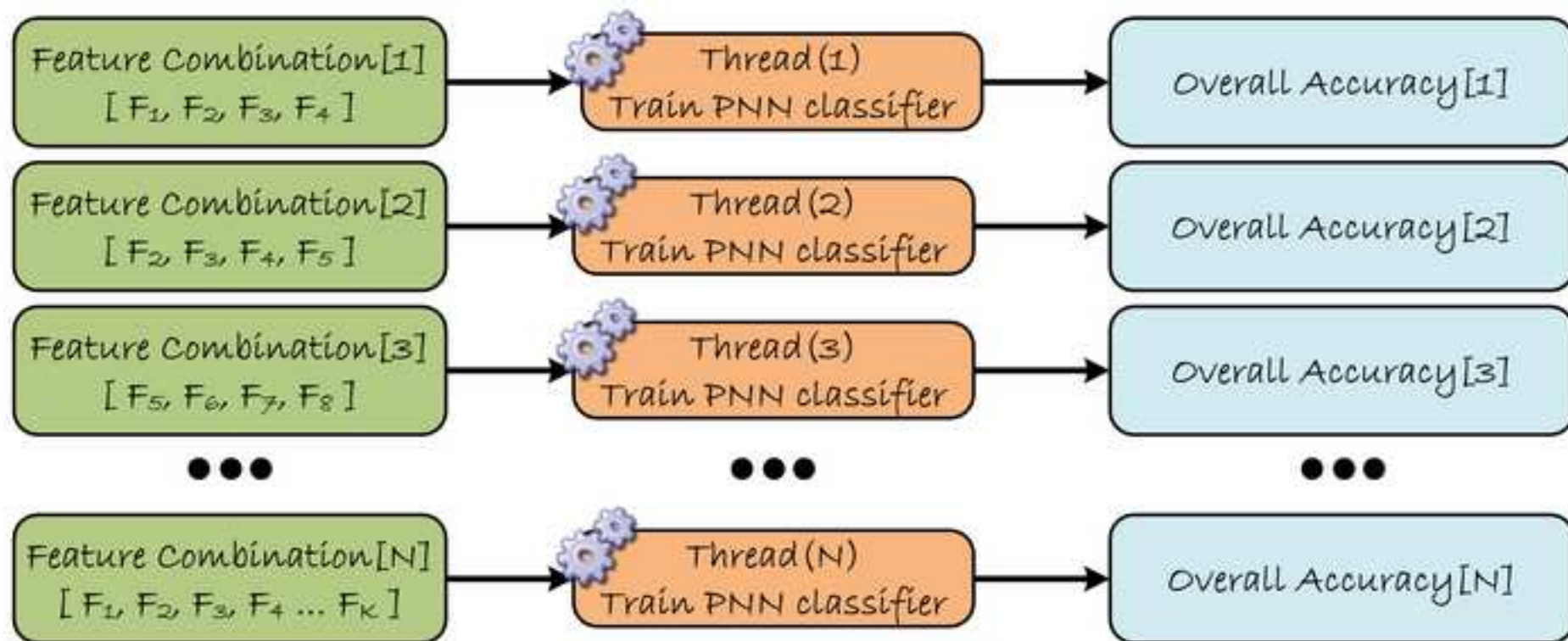


Figure 4
[Click here to download high resolution image](#)

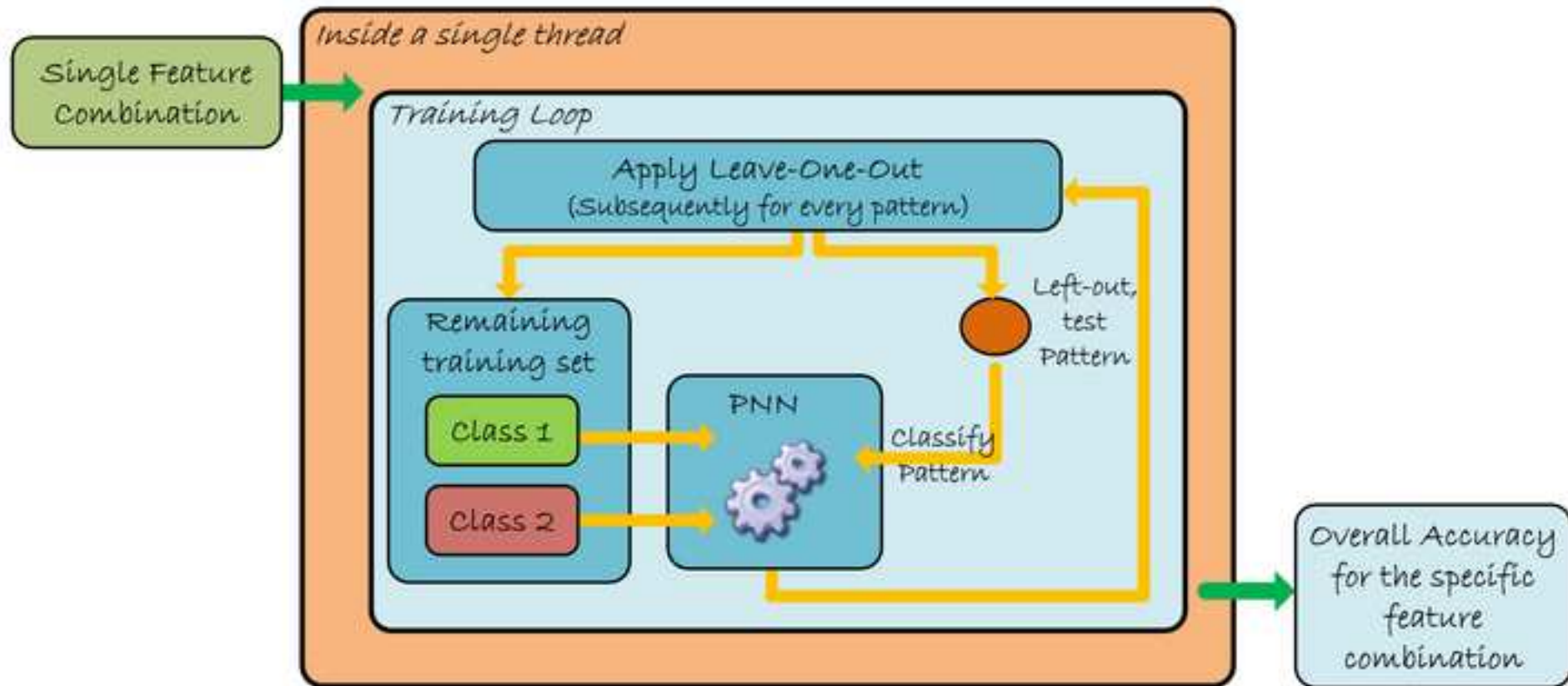


Figure 5
[Click here to download high resolution image](#)

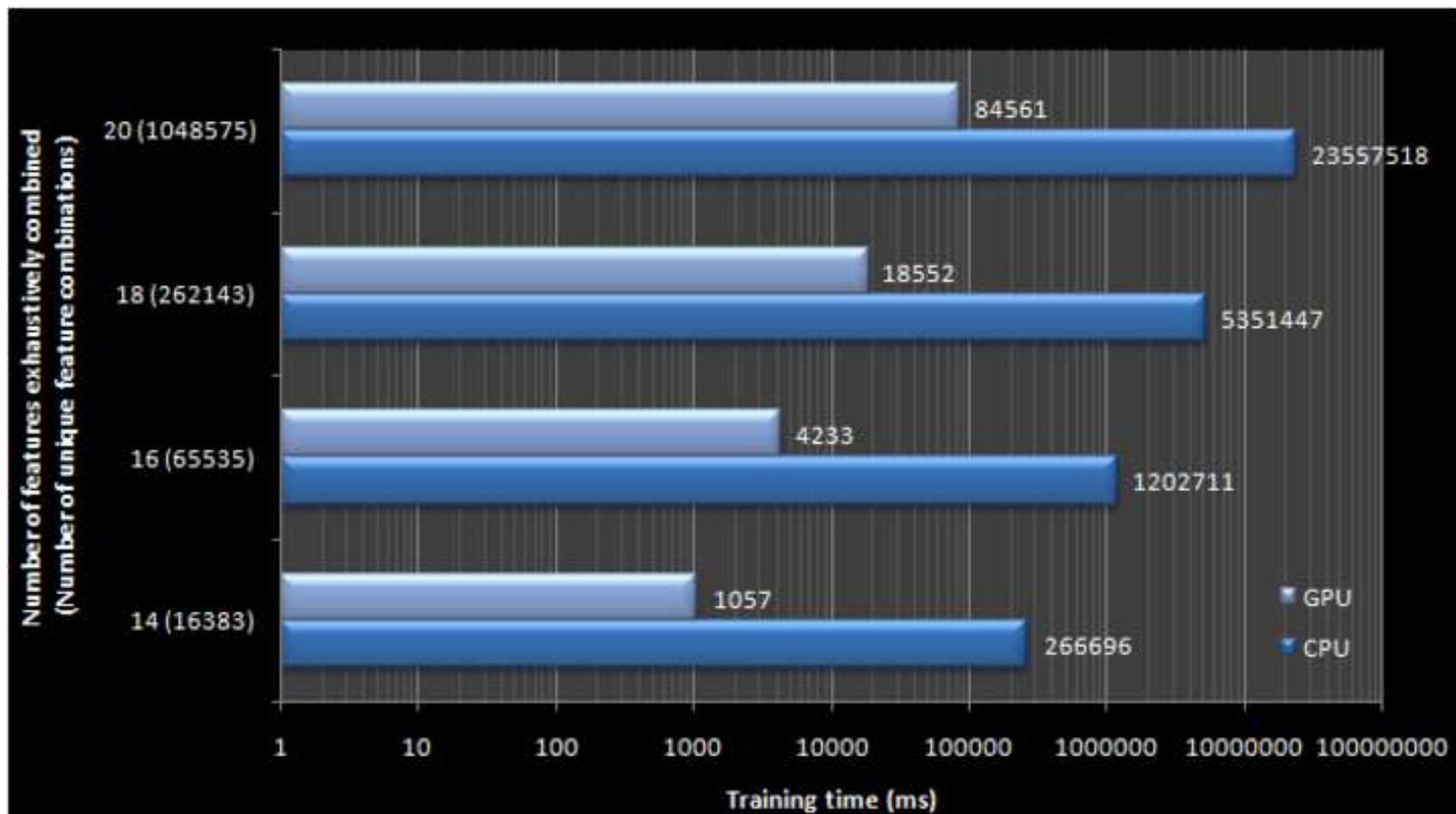


Figure 6
[Click here to download high resolution image](#)

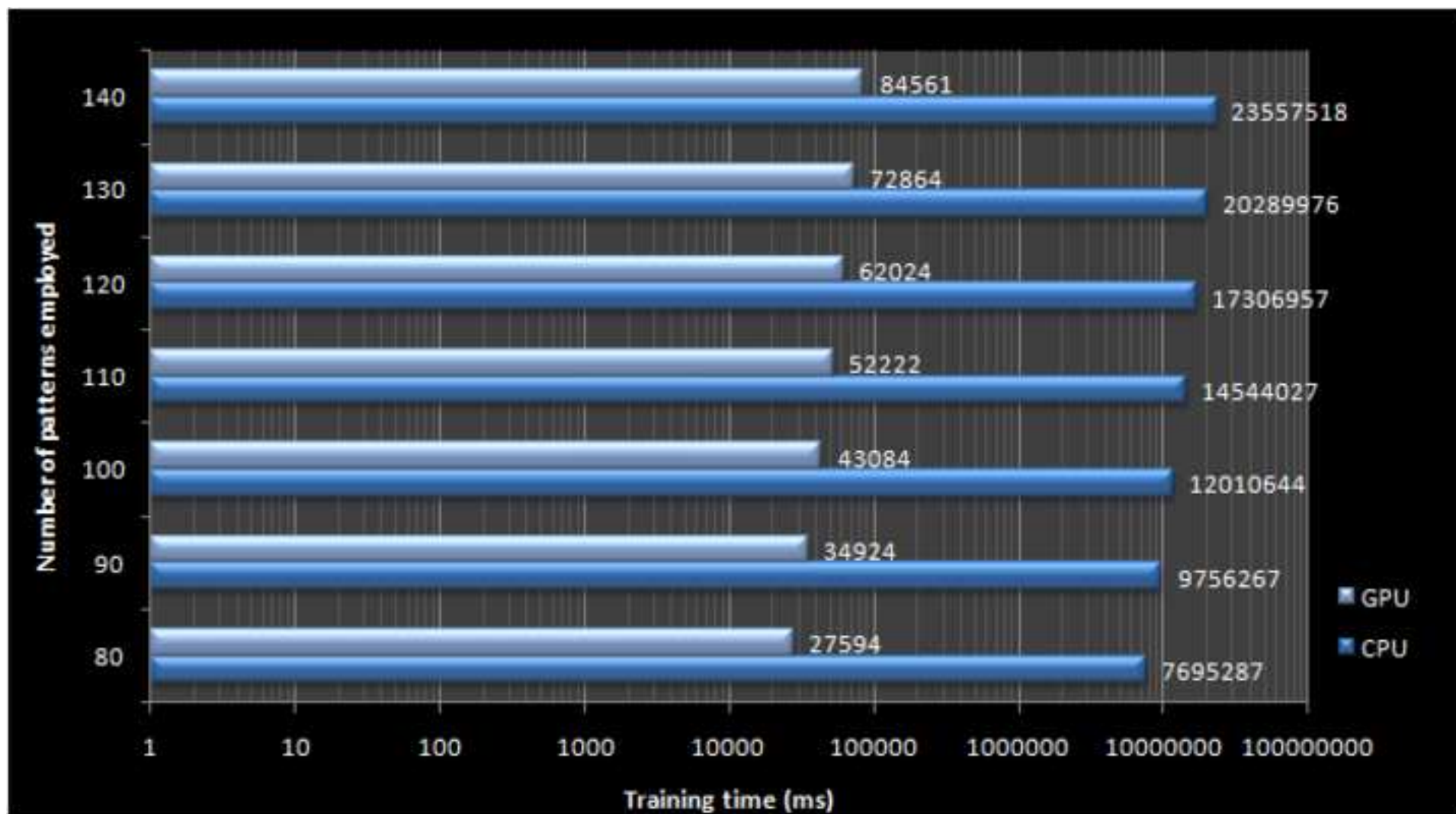
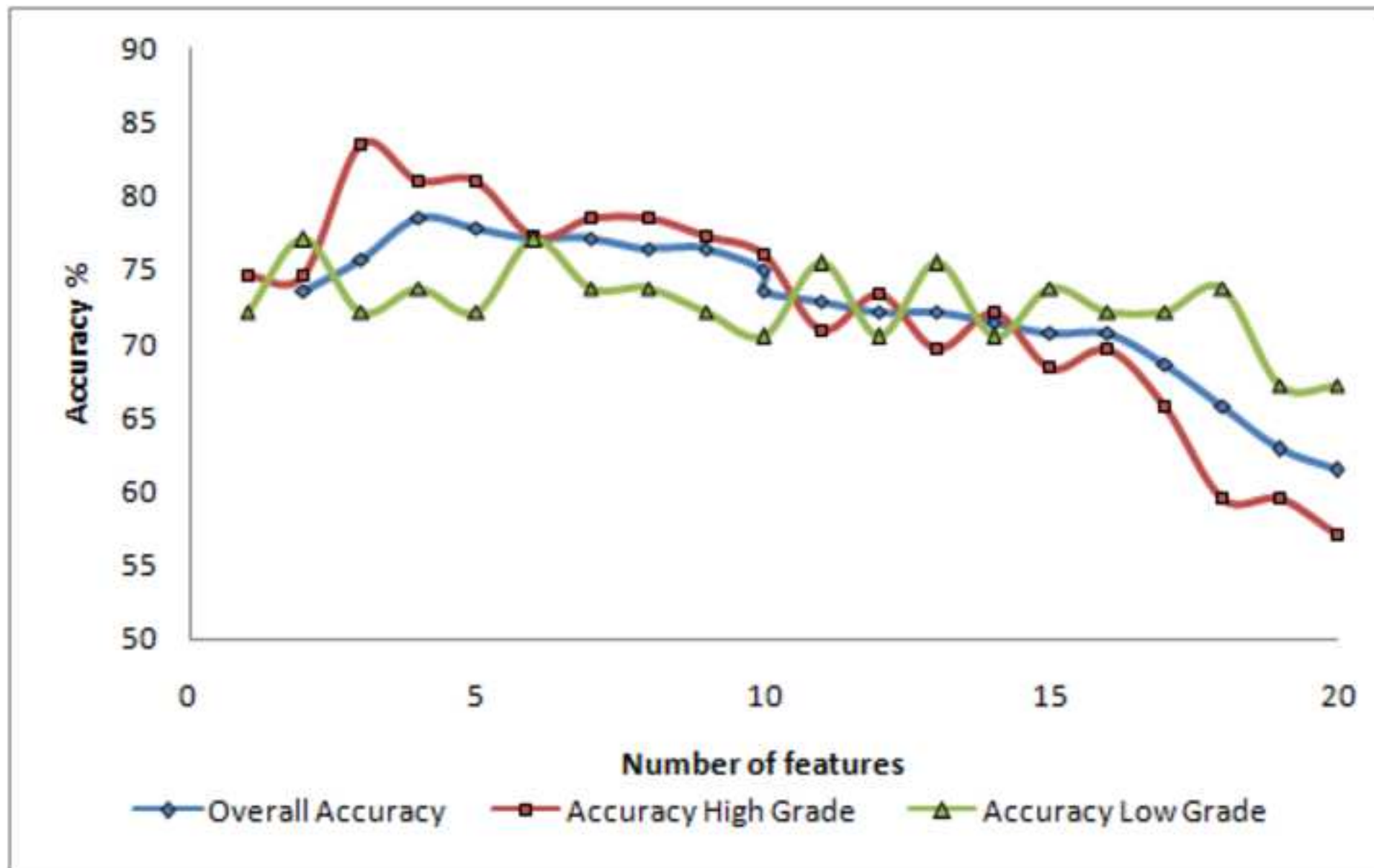


Figure 7
[Click here to download high resolution image](#)



Cover Letter

[Click here to download Supplementary Material: cover letter_sidiropoulos.doc](#)